Local Cation Coordination Motifs in Polyphosphazene Based Composite Electrolytes

Leo van Wüllen,*[,†] Thomas K.-J. Köster,[†,‡] Hans-Dieter Wiemhöfer,[§] and Nitin Kaskhedikar[§,||]

Institut für Physikalische Chemie, Westfälische Wilhelms-Universität Münster, Corrensstr. 28−30, D-48149 Münster, Germany, NRW Graduate School of Chemistry, Corrensstr. 30, D-48149 Münster, Germany, Institut für Anorganische and Analytische Chemie, Westfälische Wilhelms-Universität Münster, Corrensstr. 28−30, D-48149 Münster, Germany

Received July 7, 2008. Revised Manuscript Received October 2, 2008

Solid electrolytes in the system BMEAP/LiTf/Al_2O_3 (BMEAP = poly[(bis(2-methoxy-ethyl)-amino)$_{(2-x)}$(propylamino)$_x$]polyphosphazene; $x = 0.4$, Tf = CF_3SO_3) were studied employing a range of advanced solid state NMR methodologies including ^{7}Li-{^{1}H} CPMAS, REDOR, and ^{7}Li-{^{1}H}-CPMAS-{^{27}Al} REAPDOR NMR spectroscopy. In the binary system BMEAP/LiTf, three different ^{7}Li signals corresponding to different Li environments could be identified. Approximately 10% of the Li in the samples proved to be rather mobile with the mobility ultimately linked to the polymer dynamics, whereas 30% of the total Li content contributes to a signal which could be assigned to a Li species located within the pockets opened by the BMEA side chains as evidenced from various ^{7}Li-{^{1}H} double resonance NMR experiments such as CPMAS and REDOR NMR. The majority of the Li cations, however (ca. 62% of the Li), was found to be completely immobile, even at elevated temperatures (365 K). However, the results of ^{19}F MAS NMR experiments rule out the existence of any extended precipitates of crystalline LiTf. In the Al_2O_3-containing samples, a further Li signal could be identified by ^{7}Li-{^{1}H} CPMAS spectroscopy. This signal intensity is increasing with decreasing particle size of the added alumina. Employing ^{7}Li-{^{1}H}-CPMAS-{^{27}Al} REAPDOR NMR spectroscopy, this signal could be safely assigned to Li cations in ultimate proximity to the alumina surface. To our knowledge, this is the first direct experimental proof for such an interaction between Li cations and the alumina surface based on dipolar recoupling NMR techniques, which has been suggested as an important step in the mechanism of ion conduction in composite systems.

Introduction

The search for solid ion-conducting materials for use as solid electrolytes in all solid state batteries continues to play a dominant role in today's materials science.[1,2] Apart from a high mechanical flexibility, low weight, and electrochemical resistance predominantly a high ionic conductivity accompanied by a vanishing electronic contribution constitute the most important key properties. Especially the intrinsic low weight and high mechanic flexibility renders ion conducting polymer electrolytes promising candidates. Since the pioneering work of Wright et al.[3,4] and Armand et al.[5] a multitude of studies have been devoted to the synthesis and characterization of polymer electrolytes based on poly(ethylene oxide) (PEO). A rather important characteristic of the PEO based polymer electrolytes is their strong tendency toward crystallization and the concomitant formation of a mixture of different phases. The coordination of the Li cations in crystalline salt-in-polymer PEO based polymer electrolytes is mainly accomplished by the ether oxygen atoms, as has been shown by Bruce et al.[6−8] employing X-ray diffraction techniques. This coordination motif is also found in the amorphous polymer electrolytes, as exemplified by neutron diffraction studies employing contrast variation.[9]

Employing NMR techniques, Berthier et al.[10] could show that the ionic conductivity predominantly occurs in the amorphous parts (above the glass transition temperature T_G) of the often multiphased PEO based polymer electrolytes. Consequently, considerable effort has been devoted to suppress the crystallization within these materials, either by addition of plasticizers, the addition of cross-linkers, or the insertion of oxymethylene units into the oxyethylene polymer chain.[11−13] Although a wealth of studies have been published in which the effects of the variation of the Li salt, the nature

† Institut für Physikalische Chemie, Westfälische Wilhelms-Universität Münster.
‡ NRW Graduate School of Chemistry.
§ Institut für Anorganische and Analytische Chemie, Westfälische Wilhelms-Universität Münster.
|| Present address: Max-Planck-Institut für Festkörperforschung, Heisenbergstr. 1, D-70569 Stuttgart, Germany.

(1) Jain, H.; Thomas, J. O.; Whittingham, M. S. *MRS Bull.* **2000**, *25*, 11.
(2) Sadoway, D. R.; Mayes, A. M. *MRS Bull.* **2002**, *27*, 590.
(3) Wright, P. V. *Electrochim. Acta* **1998**, *43*, 1137.
(4) Fenton, D. E.; Parker, J. M.; Wright, P. V. *Polymer* **1973**, *14*, 589.
(5) Armand, M. B.; Duclot, M. J.; Rigaud, P. *Solid State Ionics* **1981**, *3−4*, 429.
(6) Gadjourova, Z.; Andreev, Y. G.; Tunstall, D. P.; Bruce, P. G. *Nature* **2001**, *412*, 520.
(7) Lightfoot, P.; Mehta, M. A.; Bruce, P. G. *Science* **1993**, *262*, 883.
(8) Tremayne, M.; Lightfoot, P.; Mehta, M. A.; Bruce, P. G.; Harris, K. D. M.; Shankland, K.; Gilmore, C. J.; Bricogne, G. *J. Solid State Chem.* **1992**, *100*, 191.
(9) Mao, G.; Saboungi, M. L.; Price, D. L.; Badyal, Y. S.; Fischer, H. E. *Europhys. Lett.* **2001**, *54*, 347.
(10) Berthier, C.; Gorecki, W.; Minier, M.; Armand, M. B.; Chabagno, J. M.; Rigaud, P. *Solid State Ionics* **1983**, *11*, 91.
(11) Kelly, J.; Owen, J. R.; Steele, B. C. H. *J. Power Sources* **1985**, *14*, 13.

10.1021/cm801841j CCC: $40.75
Published on Web 11/17/2008

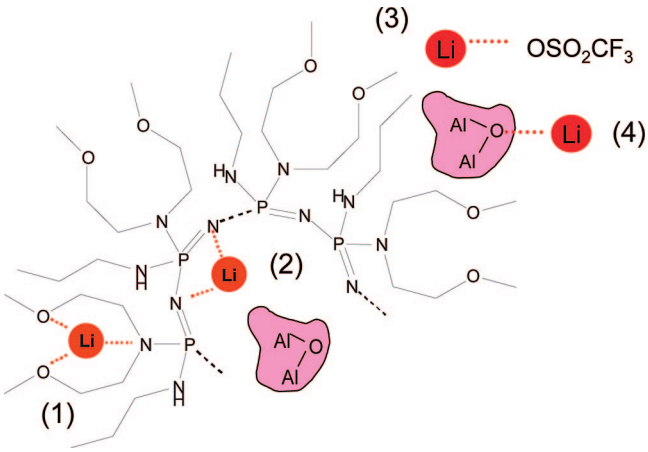

Figure 1. Coordination motifs for lithium cations in BMEAP based composite electrolytes containing alumina particles.

of the base polymer, and the cross-linking strategy have been investigated in detail, the last years have not witnessed a decisive increase in the achievable ionic conductivity. It thus seems unlikely that the ionic conductivity can be raised decisively above 10^{-5} S cm^{-1} employing conventional PEO/LiX systems.

For some years, two alternative routes toward polymer electrolytes with high ionic conductivities have been advertised. The first route involves the use of polyphosphazene (PPZ) based polymer electrolytes.[14−17] In these polymers polyether side chains are attached to the phosphorus atom of the inorganic backbone which consists of −P=N− units. The very high flexibility of the inorganic backbone entails rather low glass transition temperatures and an almost vanishing tendency to crystallize and consequently offers the promise for high ionic conductivities. Although a number of publications have appeared during the last years, no clear information about the Li coordination in these materials is available. Whereas in the salt-in-polymer PEO based systems the coordination of the Li cations almost exclusively is accomplished by the ether oxygen atoms, in the PPZ based materials the situation is far more complex. Figure 1 illustrates this for the PPZ based polymer poly[(bis(2-methoxy-ethyl)amino)$_{(2-x)}$(propylamino)$_x$]polyphosphazene (BMEAP) as an example.[18,19] Three different coordination motifs can be envisaged for the Li cations. Apart from the coordination by the BMEA oxygen atoms (1), a coordination by the nitrogen atoms of the inorganic backbone (2) may also be possible. In addition, some of the Li may be involved

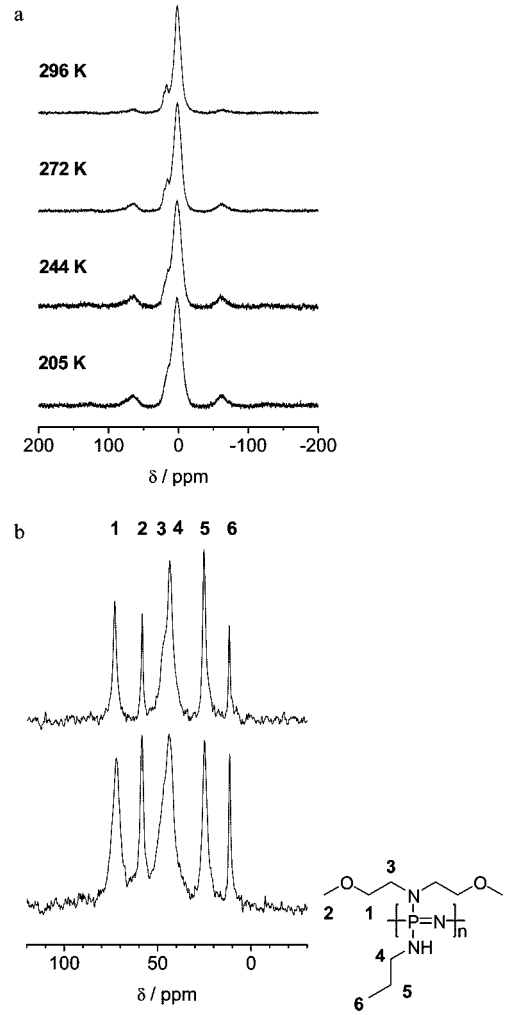

Figure 2. (a) ^{31}P MAS spectra of BMEAP/12.5/− at temperatures between 205 and 296 K. (b) ^{13}C-{^{1}H}-CPMAS spectra of pristine BMEAP (top) and BMEAP/12.5/− (bottom). The numbers indicate the assignment of the ^{13}C signals to the carbon atoms of BMEAP (see inset).

in some kind of nondissolved LiX species (ranging from contact ion pairs to extended precipitates of LiX (3).

Concerning the local Li coordination motifs in PPZ based electrolytes, the results do not seem to have converged yet. Whereas Luther and co-workers[20] propose a coordination of the Li cations by the backbone nitrogen atoms based on the results from a solution state NMR study, Allcock et al.[21] find no contribution of this basic site to the Li coordination. In a Raman study on a MEE (MEE = methoxyethoxyethoxy) based PPZ/LiTf (Tf = CF_3SO_3) polymer electrolyte Frech et al.[22] find that most of the LiTf is present in the form of ion pairs or higher aggregates and thus is not available for participating in the ionic transport.

The second route toward materials with improved ionic conductivities relies on the usage of (nanoscaled) inorganic ceramic materials such as Al_2O_3, TiO_2, or SiO_2 which are added to the polymer electrolyte, forming a composite. The

(12) Cheradame, H. LeNest, J. F. In *Polymer Electrolyte Reviews-I*; MacCallum, J. R., Vincent, C. A., Eds.; Elsevier Applied Science: New York, 1987; Chapter 5.
(13) Craven, J. R.; Mobbs, R. H.; Booth, C.; Giles, J. R. M. *Makromol. Chem., Rapid Commun.* **1986**, *7*, 81.
(14) Blonsky, P. M.; Shriver, D. F.; Austin, P.; Allcock, H. R. *J. Am. Chem. Soc.* **1984**, *106*, 6854.
(15) Allcock, H. R.; Austin, P. E.; Neenan, T. X.; Sisko, J. T.; Blonsky, P. M.; Shriver, D. F. *Macromolecules* **1986**, *19*, 1508.
(16) Paulsdorf, J.; Burjanadze, M.; Hagelschur, K.; Wiemhöfer, H.-D. *Solid State Ionics* **2004**, *169*, 25.
(17) Allcock, H. R.; Crane, C. A.; Morrissey, C. T.; Nelson, J. M.; Reeves, S. D.; Honeyman, C. H.; Manners, I. *Macromolecules* **1996**, *29*, 7740.
(18) Paulsdorf, J.; Kaskhedikar, N.; Burjanadze, M.; Obeidi, S.; Stolwijk, N. A.; Wilmer, D.; Wiemhöfer, H.-D. *Chem. Mater.* **2006**, *18*, 1281.
(19) Kaskhedikar, N.; Paulsdorf, J.; Burjanadze, M.; Karatas, Y.; Roling, B.; Wiemhöfer, H.-D. *Solid State Ionics* **2006**, *177*, 2699.
(20) Luther, T. A.; Stewart, F. F.; Budzien, J. L.; LaViolette, R. A.; Bauer, W. F.; Harrup, M. K.; Allen, C. W.; Elayan, A. *J. Phys. Chem. B* **2003**, *107*, 3168.
(21) Allcock, H. R.; Napierala, M. E.; Olmeijer, D. L.; Best, S. A.; Merz, K. M. *Macromolecules* **1999**, *32*, 732.
(22) Frech, R.; York, S.; Allcock, H.; Kellam, C. *Macromolecules* **2004**, *37*, 8699.

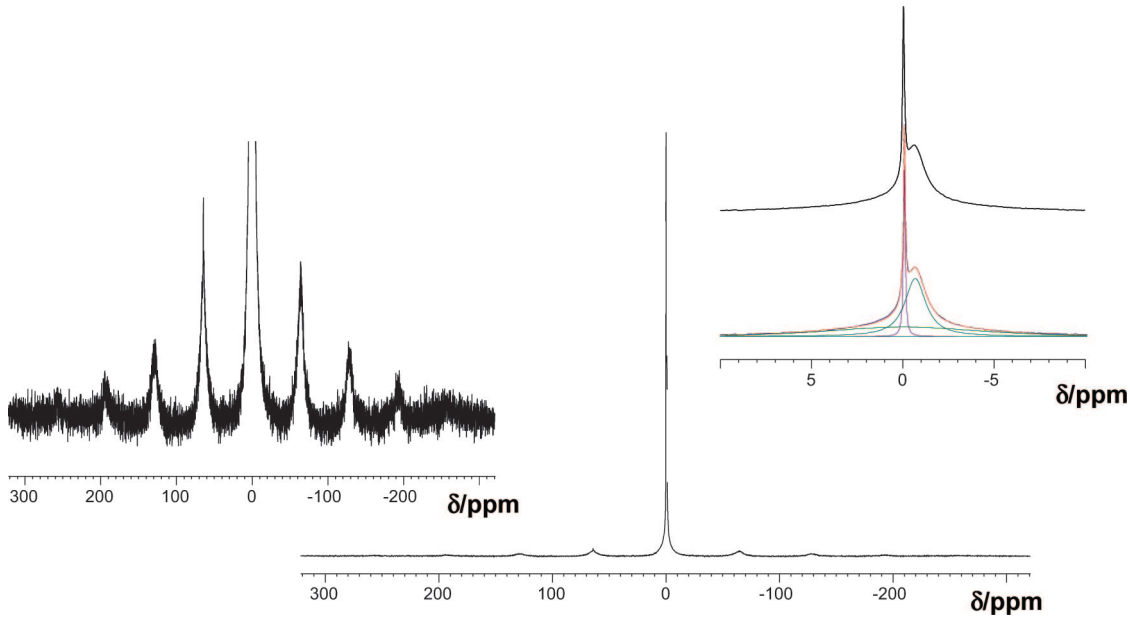

Figure 3. ^{7}Li MAS spectrum of BMEAP/12.5/−. The insert on the left shows the magnified sideband pattern, and the insert on the right shows the deconvolution of the central line into three signals.

Table 1. Deconvolution of ^{7}Li MAS Spectra of the Studied BMEAP/LiTf/Al_2O_3 Electrolytes

sample	signal	δ_{iso}, ppm	line width, Hz	rel. area, %
BMEAP/12.5/−	s	0.03	18	6.9
	b	−0.55	205	26.4
	vb	0.16	1411	66.7
BMEAP/8/10/m	s	−0.06	24	9.8
	b	−0.50	214	34.5
	vb	0.14	1600	55.7
BMEAP/8/10/n	s	−0.04	18	4.4
	b	−0.55	215	36.7
	vb	0.10	1379	58.9
BMEAP/10/10/m	s	−0.04	22	9.1
	b	−0.50	218	41.3
	vb	−0.17	1765	49.6
BMEAP/10/10/n	s	0.02	17	5.0
	b	−0.41	227	39.6
	vb	0.55	1864	55.4

first attempts to incorporate inorganic fillers into polymer electrolytes were motivated by the quest to improve the mechanical performance of the materials. The observation, that, as a side effect, the ionic conductivity increased considerably, triggered intense work in this field. Croce et al.[23,24] and others[25] find an increase in the ionic conductivity of about 1 order of magnitude when adding Al_2O_3, $LiAlO_2$, or TiO_2 to the polymer electrolyte PEO/$LiClO_4$.

A first explanation for this effect was motivated by the observation that the addition of a ceramic filler considerably diminishes the crystallization kinetics of PEO in the samples.[25−27] More elaborated studies, however, challenged this explanation. Morita et al.[28] find a drastic increase in the ionic conductivity upon $LiAlO_2$ addition to PEMM based polymer electrolytes when using $LiClO_4$ as the Li salt, contrasted to an almost vanishing effect when employing LiTf as the Li salt. In some systems a decrease in the glass transition temperature is observed, whereas in other cases no change or even an increase of this value is found. The groups of Greenbaum and Croce, employing PFG-NMR, observed an increase in the Li diffusivity in the system PEO/$LiClO_4$ upon addition of TiO_2, whereas the segment mobility of the PEO chains was found to remain unchanged.[29,30] Furthermore, Ardel[31] and Dai[32] report the existence of different cation species in LiI/Al_2O_3 mixtures in LiI/PEO based composites as they observed up to three ^{7}Li NMR signals in the corresponding MAS NMR spectra. One of these lines was tentatively assigned to ions near the alumina surface; however, these interactions were not directly analyzed.

All these observations point to the existence of significant interactions between the Li cations, the salt anions, and the polyether oxygen atoms on the one hand and the surface of the ceramic particles on the other. On the basis of these observations, several models were advertised, the space charge model,[33] electrostatic interactions[34,35] and Lewis acid−Lewis base interactions,[36−41] from which the latter has found the largest acceptance. The model is based on the assumption that the Lewis acidic and Lewis basic sites at

(23) Croce, F.; Appetecchi, G. B.; Persi, L.; Scrosati, B. *Nature* **1998**, *394*, 456.
(24) Capuano, F.; Croce, F.; Scrosati, B. *J. Electrochem. Soc.* **1991**, *138*, 1918.
(25) Siekierski, M.; Wieczorek, W.; Przyluski, J. *Electrochim. Acta* **1998**, *43*, 1339.
(26) Best, A. S.; Ferry, A.; MacFarlane, D. R.; Forsyth, M. *Solid State Ionics* **1999**, *126*, 269.
(27) Croce, F.; Scrosati, B.; Mariotto, G. *Chem. Mater.* **1992**, *4*, 1134.
(28) Morita, M.; Fujisaki, T.; Yoshimoto, N.; Ishikawa, M. *Electrochim. Acta* **2001**, *46*, 1565.
(29) Chung, S. H.; Wang, Y.; Persi, L.; Croce, F.; Greenbaum, S. G.; Scrosati, B. *J. Power Sources* **2001**, *97−98*, 644.
(30) Cheung, I. W.; Chin, K. B.; Greene, E. R.; Smart, M. C.; Abbrent, S.; Greenbaum, S. G.; Prakash, G. K. S.; Suranpudi, S. *Electrochim. Acta* **2003**, *48*, 2149.
(31) Ardel, G.; Golodnitsky, D.; Peled, E.; Wang, Y.; Wang, G.; Bajue, S.; Greenbau, S. *Solid State Ionics* **1998**, *113−115*, 477.
(32) Dai, Y.; Greenbaum, S.; Golodnitsky, D.; Ardel, G.; Strauss, E.; Peled, E.; Rosenberg, Y. *Solid State Ionics* **1998**, *106*, 25.
(33) Tambelli, C. C.; Bloise, A. C.; Rosario, A.; Pereira, E. C.; Magon, C. J.; Donoso, J. P. *Electrochim. Acta* **2002**, *47*, 1677.
(34) Best, A. S.; Adebahr, J.; Jacobsson, P.; MacFarlane, D. R.; Forsyth, M. *Macromolecules* **2001**, *34*, 4549.
(35) Singh, P. K.; Chandra, A. *J. Phys. D: Appl. Phys.* **2003**, *36*, L93.

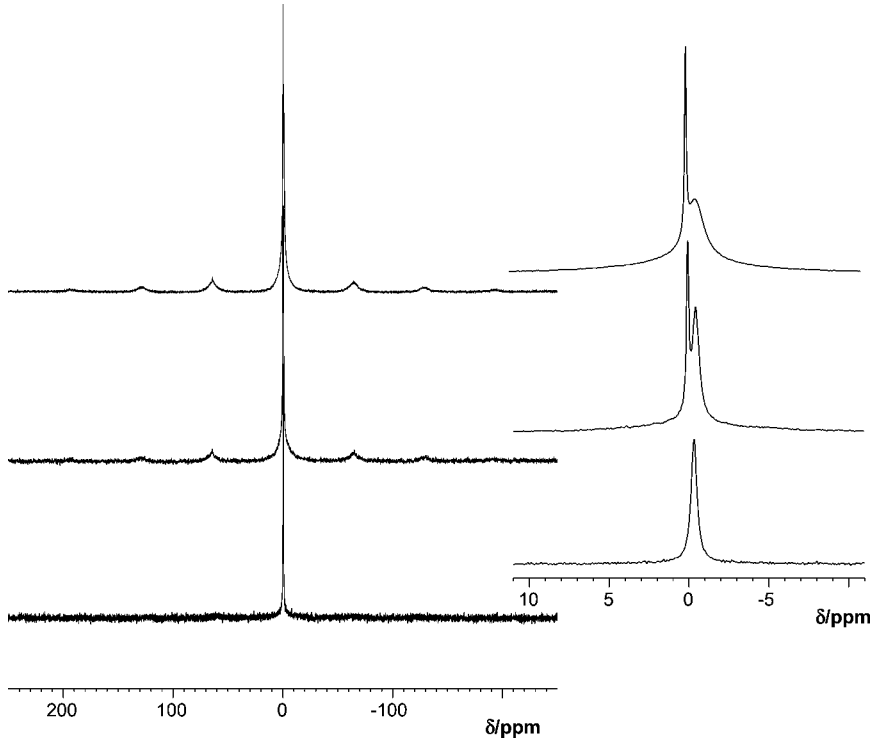

Figure 4. ^{7}Li MAS spectrum (top), ^{7}Li-{^{1}H} decoupled spectrum (middle), and ^{7}Li-{^{1}H}CPMAS spectrum of BMEAP/12.5/−. On the right the spectral region 10 ppm > δ > −10 ppm (central transition) is shown.

the surface of the ceramic particle decisively intervene with the interplay of electrostatic interactions between the present cationic (Li cations) and anionic (polyether oxygen and salt anions) ingredients. For the samples studied in this work, an increase in the ionic conductivity from 3.1×10^{-7} S/cm to 10^{-5} S/cm at room temperature has been observed upon incorporation of nanoscaled alumina.[19] Apart from this, the Li^{+} transference number was significantly raised upon addition of the alumina powder.

In this contribution we present an extended solid state NMR study to probe the local coordination motifs in PPZ based (nano)-composites of the type BMEAP/LiTf/Al_2O_3. When a range of advanced solid state NMR strategies including temperature dependent ^{7}Li and ^{19}F MAS (magic angle spinning) NMR, ^{7}Li-{^{1}H} CP (cross polarization) MAS NMR, ^{7}Li-{^{1}H} REDOR (rotational echo double resonance) NMR spectroscopy, and ^{7}Li-{^{1}H}-CPMAS-{^{27}Al} REAPDOR (rotational echo adiabatic passage double resonance) NMR spectroscopy was employed, four different local Li coordination sites could be identified and assigned. Especially the results from the latter experiment produce unequivocal proof for a distinct interaction between Li cations and the alumina surface.

(36) Wieczorek, W.; Zalewska, A.; Raducha, D.; Florjanczyk, Z.; Stevens, J. R. *J. Phys. Chem. B* **1998**, *102*, 352.
(37) Marcinek, M.; Bac, A.; Lipka, P.; Zalewska, A.; Zukowska, G.; Borkowska, R.; Wieczorek, W. *J. Phys. Chem. B* **2000**, *104*, 11088.
(38) Wieczorek, W.; Lipka, P.; Zukowska, G.; Wycislik, H. *J. Phys. Chem. B* **1998**, *102*, 6968.
(39) Wieczorek, W.; Stevens, J. R.; Florjanczyk, Z. *Solid State Ionics* **1996**, *85*, 67.
(40) Croce, F.; Persi, L.; Scrosati, B.; Serraino-Fiory, F.; Plichta, E.; Hendrickson, M. A. *Electrochim. Acta* **2001**, *46*, 2457.
(41) Jayathilaka, P.; Dissanayake, M.; Albinsson, I.; Mellander, B. E. *Electrochim. Acta* **2002**, *47*, 3257.
(42) Gullion, T.; Schäfer, J. S. *J. Magn. Reson.* **1989**, *81*, 196.

Experimental Section

The PPZ polymer poly[(bis(2-methoxy-ethyl)amino)$_{(2-x)}$(propylamino)$_x$]polyphosphazene with $x = 0.4$ [in the following abbreviated as BMEAP] was synthesized as described earlier with an average molecular weight of 10^5 D.[18,19] From this, the BMEAP/Al_2O_3/LiTf polymer electrolyte samples were prepared according to the following procedure. A total of 0.3 g of the polymeric BMEAP was dissolved in 3 mL of freshly distilled THF to obtain a clear solution. 10 (or 12.5) weight percent of lithium triflate ($LiSO_3CF_3$, purum, Fluka) was added, and the solution was stirred for 24 h. To this solution was added the desired amount of Al_2O_3 powder. In this work, Al_2O_3 in two different grain sizes was used. Samples labeled "n" were synthesized using nanoscaled γ-Al_2O_3 (40 nm, Aldrich); samples labeled "m" were prepared utilizing microcrystalline Al_2O_3 (50 μm, Aldrich). The resultant dispersion was stirred for another 24 h and then poured into a Teflon mold and sealed with parafilm, and the solvent was allowed to evaporate for 5 days. The membranes were dried in an oven at 60 °C for 48 h and in vacuum for 24 h. Throughout the text the samples are referenced to employing the following notation: BMEAP/X/Y/Z, in which X denotes the wt % of LiTf, Y the wt % of added Al_2O_3, and Z specifies the nature of the added alumina (n for nano and m for micro); thus BMEAP/10/4/n denotes a BMEAP polymer with 10 wt % LiTf and 4 wt % added nanoscaled Al_2O_3.

The NMR measurements were carried out on a BRUKER DSX 400 spectrometer with resonance frequencies of 100.7 MHz, 104.3 MHz, 155.5 MHz, 162.0 MHz, 376.6 MHz, and 400.1 MHz for ^{13}C, ^{27}Al, ^{7}Li, ^{31}P, ^{19}F, and ^{1}H, respectively. The triple resonance ^{7}Li-{^{1}H}-CPMAS-{^{27}Al}-REAPDOR NMR experiments were performed employing a BRUKER triple resonance probe.

Spectra are referenced to 1 M aqueous LiCl for ^{7}Li NMR, $CFCl_3$ for ^{19}F NMR, and 1 M aqueous $Al(NO_3)_3$ for ^{27}Al. Typically, ^{7}Li NMR spectra were recorded using acquisition delays of 30−120 s and a spinning frequency of 10 kHz; for ^{19}F NMR spectra delays of 20 s and spinning rates of 10 kHz were used. The spectra were

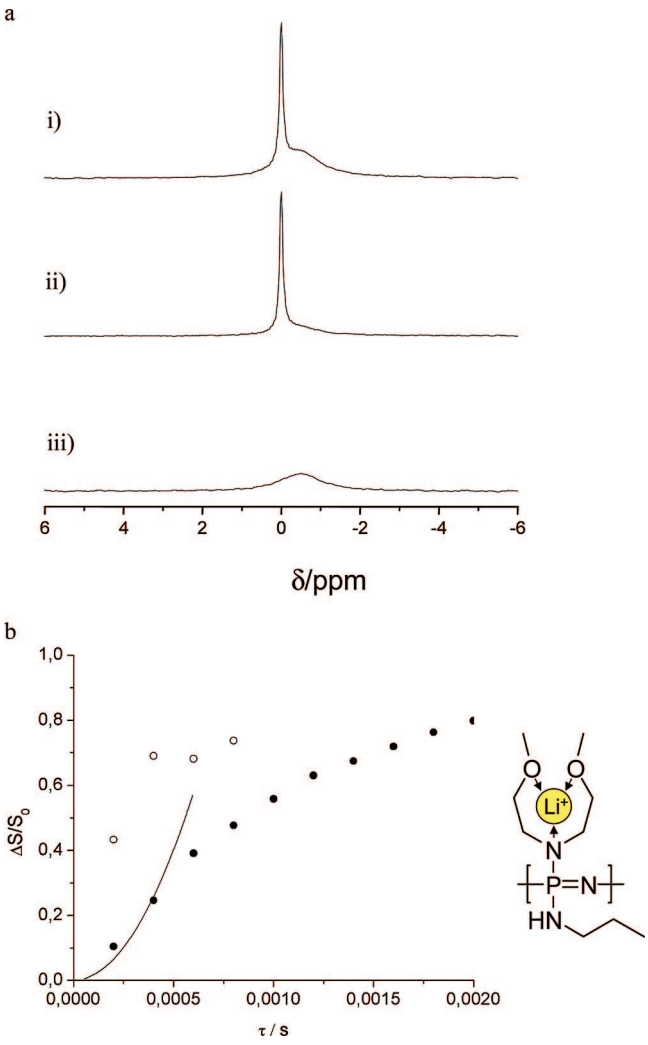

Figure 5. (a, i) ^{7}Li spin echo spectrum (S_0), (ii) ^{7}Li-{^{1}H} REDOR signal (S), and (iii) signal difference $\Delta S = S_0 - S$ for BMEAP/12.5/− at 295 K. The resulting REDOR curves for signal (b) at −0.55 ppm are plotted in (b), where data points at 295 K are represented by filled black circles and data points for $T = 203$ K are marked by open black circles. The solid line shows a parabolic fit used for the evaluation of the second moment. The coordination of lithium ions by BMEA is illustrated in the insert on the right.

fitted and analyzed using the DMFIT software. The ^{7}Li-{^{1}H}-CPMAS-{^{27}Al}-REAPDOR NMR experiments were accumulated with a repetition time of 8 s with MAS being performed at 10 kHz.

The temperature dependent NMR measurements were always performed on fresh samples which were not used for temperature dependent experiments before, to exclude any bias due to thermal history.

Results and Discussion

Characterization of the Polymer Matrix. The PPZ polymer matrix was characterized employing ^{31}P MAS and ^{13}C-{^{1}H} CPMAS NMR. The ^{31}P MAS NMR spectra for the various samples were found to be virtually identical; the spectra for sample BMEAP/12.5/− are shown as a representative example in Figure 2a. Two different signals can be identified. The dominant signal at 1.5 ppm, comprising 87% of the total signal intensity, can be assigned to phosphorus nuclei located within the phosphazene chains. As in the solution state NMR for BMEAP,[18] the three different phosphorus species contributing to this signal (permutations of the two different substitutents) are not resolvable in the solid state. The shoulder at 17 ppm (ca. 13% of the total signal intensity) may be assigned to fully substituted cyclotriphosphazenes, in agreement with the corresponding solution state NMR.[18] Upon cooling, the line width of the signal at 1.5 ppm is gradually increasing from approximately 1700 Hz at room temperature to 2400 Hz at 205 K. This increase is accompanied by a gradual increase in the spinning sideband intensity, both reflecting the reduced mobility of the polymer network upon cooling ($T_G = 233$ K).

In the ^{13}C{^{1}H} CPMAS NMR spectra for all studied samples six different signals can be identified. These signals can be assigned to the individual carbon positions within the propyl-amine and BMEA substituents of the PPZ chain (cf. inset in Figure 2b). Comparing the line widths for the individual lines in the spectra of sample BMEAP/12.5/− (lower spectrum in Figure 2b) and pristine BMEAP (upper spectrum in Figure 2b), a broadening of the signals especially for carbon positions 1 and 3 of BMEA can be observed upon LiTf incorporation into the PPZ. This broadening may indicate an interaction between Li cations and the BMEA residues as discussed below in further detail.

Local Lithium Coordination Motives. The local Li coordination motives and environments were investigated employing ^{7}Li MAS NMR. Interestingly, the appearance of the spectra seems to be virtually independent of the nature or presence of alumina as ceramic filler. The spectra for all of the studied samples are characterized by a superposition of three different signals (cf. Figure 3, in which the ^{7}Li MAS NMR data for sample BMEAP/12.5/− is collected): a rather narrow signal around 0.0 ppm (denoted (s)) with a MAS line width of only 20 Hz (relative fraction 10−15%); a signal at −0.55 ppm (denoted (b), line width = 210 Hz), consuming approximately 30% of the total signal intensity, and a very broad signal (denoted (vb), line width approximately 1500 Hz), comprising approximately 60% of the total signal intensity and dominating the spinning side bands (cf. left inset of Figure 3). This broad signal is still present at temperatures up to 365 K (data not shown), indicating that the corresponding ions remain immobile even at elevated temperatures. In Table 1, a compilation of the exact chemical shift values and relative areas of the three different signals for all of the measured samples can be found. For binary BMEAP/LiTf samples, the relative fraction of the very broad component was found to increase linearly with the LiTf content of the samples, increasing from approximately 35% for samples with 5% LiTf to approximately 65% for samples with 15% LiTf. (data not shown). It is important to note that the chemical shift values and line widths for all of these three identified components are distinctively different from the ^{7}Li MAS NMR signal for pristine Li-triflate (not shown), identifying all three signals as arising from new local environments for Li cations within the PPZ/LiTf system.

To further investigate the nature of the identified Li species in the PPZ/LiTf sample, ^{7}Li MAS NMR spectra with strong ^{1}H decoupling and ^{7}Li-{^{1}H} CPMAS NMR experiments were performed. Since the ^{1}H−^{7}Li dipolar coupling usually

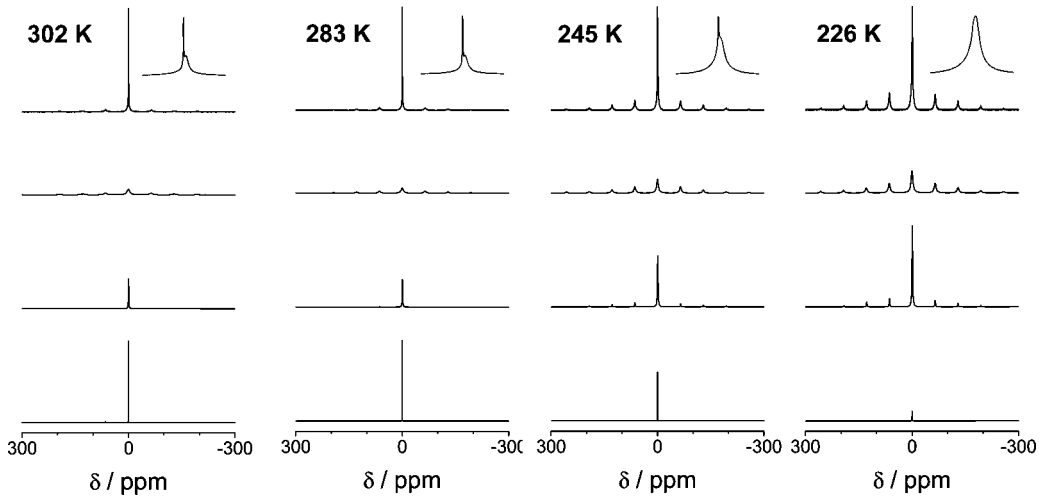

Figure 6. ^{7}Li MAS NMR spectra of BMEAP/12.5/− at 302, 283, 245, and 226 K (top). The region of the central transition (10 ppm > δ > −10 ppm) is again shown in a magnified view in the inserts. Below the spectra, the deconvolution of the spectra into the signals (vb), (b), and (s) is shown.

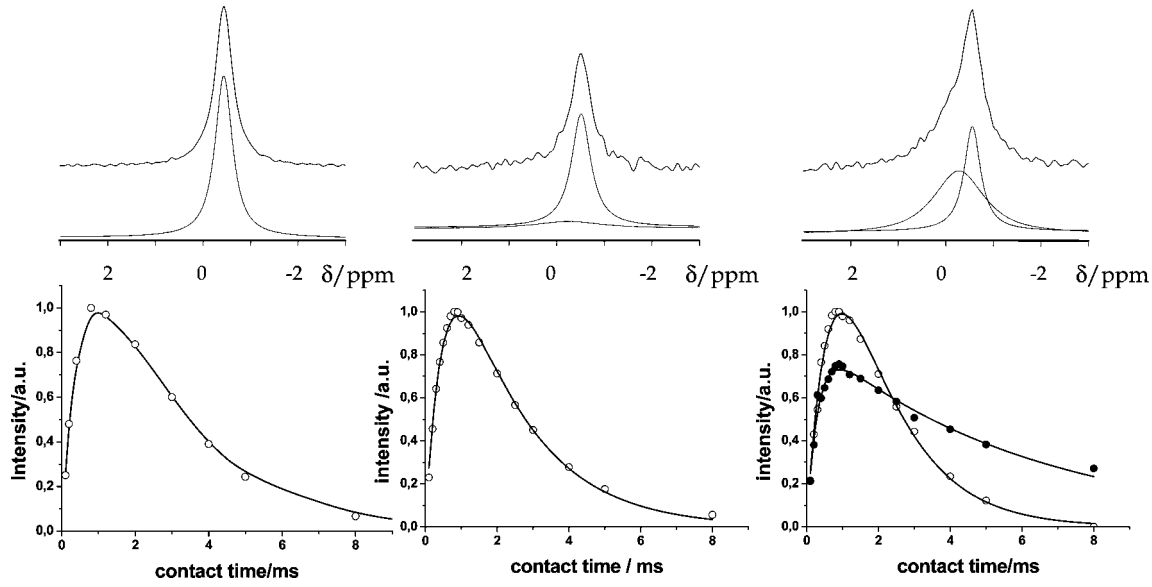

Figure 7. (a) ^{7}Li-{^{1}H} CPMAS spectra of BMEAP/12.5/−, BMEAP/8/10/m, and BMEAP/8/10/n recorded with a contact time of 5 ms together with the deconvolution into two signals. (b) Contact time behavior (signal intensity versus contact time) of the two signals; filled circles represent the NMR line at −0.27 ppm, open circles represent the line at −0.55 ppm. Solid lines are guides to the eye only.

is not completely averaged out by the MAS process, strong ^{1}H decoupling is expected to induce further line narrowing for ^{7}Li signals from Li nuclei in close proximity to protons. At the same time, exclusively these Li nuclei can be detected following a magnetization transfer step from ^{1}H to ^{7}Li in a ^{7}Li-{^{1}H} CPMAS experiment. In Figure 4, the spectra for sample BMEAP/12.5/−, obtained employing ^{7}Li MAS NMR, ^{7}Li MAS NMR with strong ^{1}H decoupling, and ^{7}Li{^{1}H} CPMAS NMR are collected. Again, no obvious differences between the spectra from alumina free and alumina containing samples can be observed. As can be inferred from an inspection of this figure, signal (b) at −0.55 ppm obviously represents Li cations in rather close proximity to protons. The line width of this signal reduces from 205 to 89 Hz upon ^{1}H decoupling and proves to be the only signal detectable in the CPMAS experiment. Contrasted to this, neither the narrow signal at 0 ppm (s) nor the broad signal (vb) seems to be affected by the ^{1}H decoupling or CP process. Together with the observation of a broadening of the ^{13}C signals associated with the BMEA carbon atoms upon LiTf addition to the polymer, this renders an assignment of the −0.55 ppm signal to Li cations associated with the BMEA-residues likely.

To further characterize the local environment of the Li cations represented by the signal at −0.55 ppm and to obtain a more quantitative measure of the ^{1}H−^{7}Li dipolar coupling, the experiments were complemented by ^{7}Li-{^{1}H} REDOR NMR experiments. Principally, the results from a rotor-synchronized spin−echo experiment for the observed (S) nuclei, defining the full echo intensity S_0, are compared to spectra resulting from an experiment in which the hetero-nuclear dipolar coupling between nuclei S and I has been reintroduced by the action of rotor-synchronized π-pulses (I-channel) in addition to the S-spin spin echo pulses (signal intensity S).[42] The difference of the spectra from the two

(43) Bertmer, M.; Eckert, H. *Solid State Nucl. Magn. Reson.* **1999**, *15*, 139.

experiments then only contains contributions from S nuclei experiencing a dipolar coupling to I nuclei. The magnitude of the REDOR effect depends on the strength of the dipolar coupling and the dipolar evolution time, the latter of which can be controlled by the number of rotor cycles and the spinning frequency. Figure 5a represents the results of a typical ^{7}Li-{^{1}H} REDOR NMR experiment for sample BMEAP/12.5/−, recorded at a dipolar evolution time of 1.2 ms. Spectrum (i) constitutes the ^{7}Li MAS spin echo spectrum, whereas (ii) was obtained utilizing ^{7}Li-{^{1}H} REDOR NMR; (iii) represents the difference of the two. The normalized difference intensity $\Delta S/S_0$ as a function of the dipolar evolution time is plotted in Figure 5b. Filled black circles represent the results of a ^{7}Li-{^{1}H} REDOR NMR experiment performed at room temperature, whereas open black circles denote the results from the corresponding experiment performed at 203 K. Since the initial slope of the dipolar evolution curves scales with the strength of the ^{7}Li−^{1}H heteronuclear dipolar coupling, the REDOR curves in Figure 5b clearly demonstrate that the effective heteronuclear dipole coupling at $T = 203$ K proves to be considerably higher than for the $T = 295$ K experiment. Obviously, the ^{7}Li−^{1}H dipolar coupling is partially averaged at room temperature due to motion. Simulations of the REDOR curves at short evolution times can be performed employing the second moment analysis introduced by Eckert and co-workers[43] using a parabolic fit to the data

$$\frac{\Delta S}{S_0} = \frac{4}{3\pi^2} M_2 \tau^2$$

in which M_2 denotes the van Vleck second moment, which can be related to the present ^{7}Li−^{1}H dipolar couplings (assuming n H neighbors) to first order by

$$M_2 = \frac{4}{15} 4\pi^2 I(I+1) \sum_{i=1}^{n} D_i^2$$

Since such an analysis is usually restricted to the regime $\Delta S/S_0 < 0.3$, the data for $T = 203$ K can only be analyzed qualitatively. The room temperature data, on the other hand, is biased by the averaging due to motion, and the resulting M_2 value can thus be taken just as a limiting lower value. The resulting values are $M_2 = 1.3 \times 10^7$ rad^2 s^{-2} at $T = 295$ K, corresponding to 3 ^{1}H nuclei in a 4 Å sphere around the central ^{7}Li nucleus and $M_2 \approx 5 \times 10^7$ rad^2 s^{-2} at $T = 203$ K, translating into 5−6 ^{1}H nuclei in a 3.5 Å sphere around the central ^{7}Li nucleus. These values can only be conceived if we assume that these Li cations are located within the pockets built by the BMEA side chains as sketched in the inset of Figure 5. The motional process which averages the Li−H dipolar coupling presumably involves the chain motion of the PPZ chains superimposed by an additional localized motional process of the BMEA residues.

The freezing of this motional process is also manifesting itself in the temperature dependence of the ^{7}Li MAS NMR spectra, shown in Figure 6. For the Li signal assigned to Li cations coordinated by the BMEA residues, signal (b) at −0.55 ppm, a gradual increase in the line width of the central signal and spinning sideband intensity is observed upon cooling. This corroborates the conclusions drawn from the ^{7}Li-{^{1}H} REDOR NMR experiment discussed above. The ^{7}Li−^{1}H dipolar coupling is partially averaged at room temperature due to the motional processes discussed above, leading to a narrow ^{7}Li MAS NMR signal without any extended spinning sideband intensity. Upon cooling, the ^{7}Li−^{1}H dipolar coupling is no longer averaged by the motional process, consequently leading to a broadening of the NMR signal and the appearance of spinning sideband intensity.

For the temperature dependence of the narrow signal (s) a slightly different behavior is observed. A broadening of the ^{7}Li MAS NMR line is only observed when cooling the investigated signals below the glass transition temperature T_G (ca. 230 K). This identifies the corresponding Li cations as members of a mobile Li species with its mobility ultimately linked to that of the PPZ polymer chain dynamics. Contrasted to this, for the very broad signal (vb) the line width of the center signal and the relative spinning sideband intensity proves to be virtually independent of temperature. Thus, this signal corresponds to a lithium species not experiencing any mobility at room temperature.

The data presented and discussed so far do not contain any manifestations of the presence or nature of the added alumina. Thus, there seems to be, at the most, a rather marginal fraction of Li cations in proximity to the Al_2O_3 surface. Nonetheless, since such a Li−alumina surface interaction has been discussed as an important ingredient to a modified conduction mechanism within the polymer electrolytes as extra hopping sites,[41] an unequivocal identification of such a species presents one of the ultimate goals of the present study. Since at the alumina surface we can expect some proton density (e.g., from Al−(OH)−Al or terminal Al−OH units), ^{7}Li-{^{1}H} CPMAS NMR spectroscopy under variation of the contact time holds the most promise to detect such a species. The corresponding ^{7}Li-{^{1}H} CPMAS NMR spectra for samples BMEAP/12.5/−, BMEAP/8/10/m, and BMEAP/8/10/n are collected in Figure 7a. Evidently, a new signal at −0.27 ppm, which is not observed in the binary samples, can be detected in the alumina containing samples at long contact times. The intensity of this new line is considerably increased for the samples containing nanoscaled Al_2O_3 (cf. Figure 7). Since the intensity of the ^{7}Li-{^{1}H} CP signal delicately depends on the relaxation times $T_{1\rho}$(Li) and $T_{1\rho}$(H) and thus on the local environment of the respective Li cation, the dependence of the corresponding signal intensity on the contact time can be taken as a fingerprint of the local environment for the detected nucleus. The contact time dependence for the signal at −0.55 ppm (occurring in all samples) proves to be identical in all measured samples with its maximum intensity occurring at a contact time of 1.2 ms. This identical contact time behavior corroborates the existence of Li cations located in the BMEA pockets (cf. Figure 6) in all the investigated samples.

In contrast, the corresponding curve for the signal at −0.27 ppm (occurring exclusively in Al_2O_3 containing samples) exhibits a distinctively different behavior. The contact time dependence observed for the signal at −0.27 ppm on the other hand exactly resembles that of a Li signal in a binary

(44) van Wüllen, L. Köster, T. K.-J. *Solid State Ionics*, in preparation.

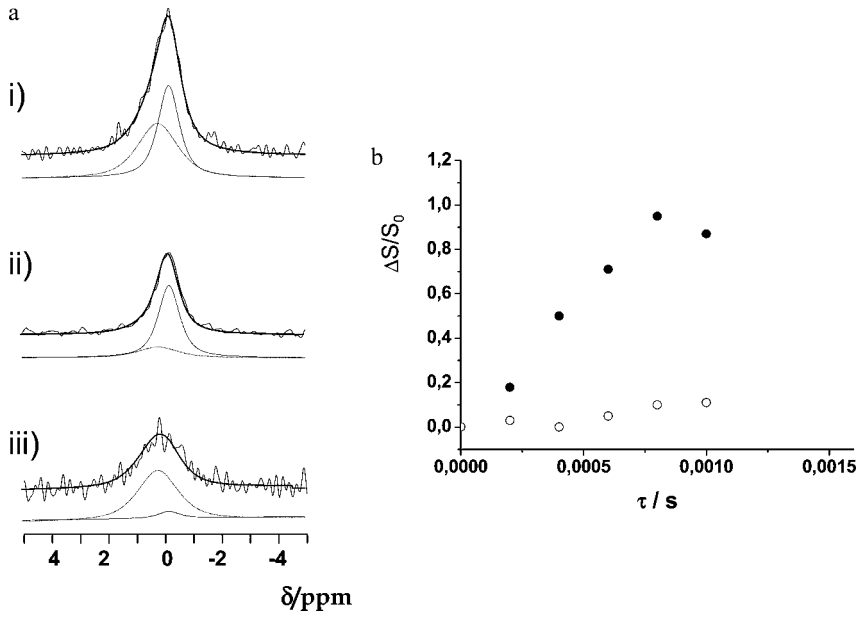

Figure 8. a): i) ^{7}Li-{^{1}H} CPMAS spin echo spectrum (S_0), ii) ^{7}Li-{^{1}H}-CPMAS-{^{27}Al} REAPDOR spectrum (S), and iii) signal difference ($\Delta S = S_0 - S$) for sample BMEAP/8/10n. The resulting REAPDOR curves are plotted in b) as a function of dipolar evolution time. Filled circles represent the line at −0.27 ppm; open circles represent the line at −0.55 ppm.

LiTf/Al_2O_3 sample[44] which could unequivocally be assigned to a Li species in rather close proximity to the alumina surface. From this observation we conclude that this new line detected in the ternary BMEAP/LiTf/Al_2O_3 samples originates in Li cations associated with the Al_2O_3 surface.

A direct proof for such a Li cation interaction with the Al_2O_3 surface involves the evaluation of the ^{7}Li-^{27}Al dipolar coupling employing ^{7}Li-{^{27}Al} REAPDOR (rotational echo adiabatic passage double resonance) NMR spectroscopy. In REAPDOR, a variation of REDOR spectroscopy optimized for quadrupolar nuclei as the dephasing nuclei, the dipolar coupling is reintroduced by the action of an adiabatic pulse of width $\tau_R/3$ for ^{27}Al. Like in REDOR, a plot of $\Delta S = S_0 - S$ as a function of evolution time τ allows the analysis of the heteronuclear dipolar coupling. Since in our case the corresponding Li signal can only be observed employing ^{7}Li-{^{1}H} CPMAS NMR spectroscopy, the ^{7}Li-{^{27}Al} REAPDOR has to be precedented by a ^{1}H-^{7}Li magnetization transfer step. The results of such an experiment, that is, a ^{7}Li-{^{1}H}-CPMAS-{^{27}Al} REAPDOR NMR experiment, are collected in Figure 8. The arrangement of the spectra in Figure 8 resembles that of those in Figure 5. Since only the −0.27 ppm signal is contributing considerably to the difference signal plotted as the lower spectrum in Figure 8a, it is clear that the Li cations contributing to this signal are experiencing a sizable dipolar coupling to ^{27}Al nuclei, whereas for the Li cations contributing to the −0.55 ppm signal (assigned to Li species located within the pockets offered by the BMEA residues) no spatial proximity to the Al_2O_3 surface can be found. Although the lithium ions near the alumina surface are not highly mobile, they may play an important role in the ion transport in composite electrolytes. In particular, the ceramic particles offer additional coordination sites for lithium ions which may contribute in the overall ion conduction.

Characterization of the Triflate Anions. The various NMR experiments tracing the location and state of the Li cations were complemented by temperature dependent ^{19}F MAS NMR studies on all samples to obtain information about the dynamic state of the anions. Again, no distinct differences were observed in the ^{19}F MAS NMR spectra for the various samples. Figure 9 presents the corresponding spectra for sample BMEAP/12.5/− as an example; the ^{19}F MAS NMR spectrum of pristine LiTf at room temperature is reproduced for comparison. Principally, the ^{19}F MAS NMR spectra of CF_3 groups are dominated by the combined effects of CSA (chemical shift anisotropy, characterized by the value $\Delta\sigma = \sigma_{33} - 0.5(\sigma_{11} + \sigma_{22})$ with σ_{xx} denoting the principal values of the CSA tensor) and homonuclear dipolar coupling. The ^{19}F MAS NMR spectrum of pristine LiTf is compatible with the assumption of a rapidly reorienting CF_3 group within an otherwise static triflate anion.[45] For the triflate anion within the BMEAP/12.5/− sample, such a situation is only found at temperatures below 233 K. For temperatures above 233 K, a gradual decrease in the spinning sideband intensity can be observed. The spectra can be simulated by a superposition of two signals: a ^{19}F signal with a $\Delta\sigma$ value of approximately 50 ppm and a second signal with an almost vanishing CSA ($\Delta\sigma$ < 17 ppm). At 295 K, the second signal comprises approximately 80% of the total signal intensity. From this it can be concluded that in the BMEAP samples the majority of the triflate anions are mobile already at $T = 273$ K.

Contrasting this observation to the results of the ^{7}Li NMR experiment, from which approximately 2/3 of the total Li cations were found to be immobile, the ^{19}F NMR results thus rule out the existence of larger precipitates of crystalline LiTf. Since, however, we cannot discriminate between the effects of an isotropic rotational diffusion of the triflate anions and an isotropic translational motion, the two observations can be reconciled assuming larger aggregates of noncrystalline LiTf units, in which at ambient temperatures the free

(45) Köster, T. K.-J.; van Wüllen, L. *Solid State Ionics* **2008**, *178*, 1879.

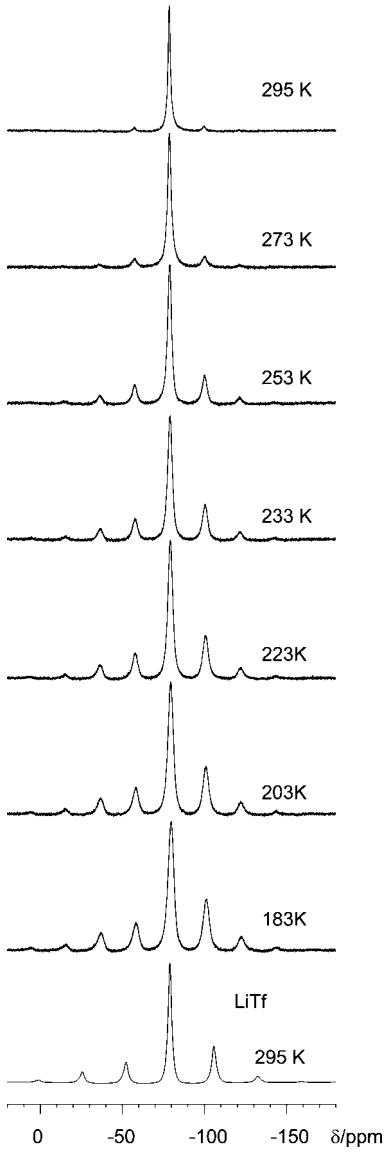

Figure 9. [19]The spectrum of pure LiTf (bottom) is shown for comparison.

volume for the anions is large enough for a low-activated isotropic rotational diffusion but the thermal energy still being too low to stimulate Li cation hopping within these aggregates.

Conclusions

The combined results from a variety of different solid state NMR approaches provide a detailed insight into the local coordination motives for the various types of Li cations within the PPZ based composite polymer electrolytes. In total, four different ^{7}Li signals could be identified: (1) Employing ^{7}Li-{^{1}H} CPMAS NMR, ^{7}Li MAS NMR with ^{1}H decoupling and ^{7}Li-{^{1}H} REDOR NMR, the ^{7}Li NMR signal at −0.55 ppm, contributing approximately 25% to the total signal intensity, could be safely assigned to Li cations which are coordinated by the BMEA residues of the PPZ. From the temperature dependence of this signal and from temperature dependent ^{7}Li-{^{1}H} REDOR NMR experiments it was concluded that these groups perform some kind of localized motion at room temperature (in addition to the PPZ chain dynamics) which is then frozen upon cooling. (2) A total of 10−15% of the Li cations within the polymer electrolytes constitute a rather mobile species. The mobility of this species was found to be linked to the glass transition temperature of the polymer. We tentatively assign these cations to be loosely connected to the PPZ polymer backbone, possibly via an interaction to the basic nitrogen sites, as suggested by Luther et al.[20] It may be possible to identify such an interaction at low temperature employing ^{15}N−^{7}Li dipolar NMR techniques on ^{15}N labeled samples in the future. Work to this end is currently in progress in our laboratories. (3) Approximately 2/3 of the total Li cations contribute to a rather broad signal, which does not experience any line shape changes upon ^{1}H decoupling and cannot be detected in a ^{7}Li-{^{1}H} CPMAS experiment. As evidenced by temperature dependent ^{7}Li MAS NMR spectroscopy the Li cations contributing to this signal are completely immobile at ambient temperatures and are thus not available for ionic transport. Since the corresponding ^{7}Li signal does not exhibit any CP or decoupling effect and the line shape and spinning sideband intensity proved to be virtually independent of temperature, these Li cations cannot be coordinated by the PPZ side chains (BMEA residues) or in some way connected to the PPZ backbone. We therefore have to assign these Li cations as part of larger "LiTf" agglomerates. Since from the ^{19}F MAS NMR data we can clearly exclude any extended crystalline LiTf precipitates, we have to assume the existence of an amorphous LiTf phase in which (at room temperature) the triflate anions are free to perform an isotropic rotational diffusion process, but the temperature is not sufficiently high to allow for Li motion within this phase. At lower temperatures then the rotational diffusive motion of the triflate anions gradually ceases.

Principally, the cations in these "LiTf" agglomerates might act as an ionic reservoir. However, the fact that we do not observe any exchange between the different Li species in the ^{7}Li MAS NMR spectra, even at elevated temperatures, renders such an exchange of Li ions among the various Li sites unlikely. (4) The fourth Li species is only present in the Al_2O_3 containing samples with its intensity being inversely proportional to the grain size of the added alumina. From ^{7}Li-{^{1}H} CPMAS and ^{7}Li-{^{1}H}-CPMAS-{^{27}Al} REAPDOR NMR experiments this Li species could be unequivocally identified as being coordinated to the alumina surface. To our knowledge this marks the first experimental proof for such an interaction, which is directly based on the evaluation of heteronuclear dipolar couplings. Since the ionic conductivities in these samples were found to drastically increase upon addition of nanoscaled alumina, our findings clearly support the model of Lewis base Lewis acid interaction as introduced by Wieczorek and Croce.[36−41]

Acknowledgment. Financial support by the Deutsche Forschungsgemeinschaft DFG (SFB 458) is gratefully acknowledged. T.K.-J.K. and N.K. thank the NRW International Graduate School of Chemistry. T.K.-J.K. also thanks the Fonds der Chemischen Industrie for a doctoral stipend.

CM801841J